

A comparative study on particle–fluid interactions in micro and nanofluids of aluminium oxide

J. Hemalatha · T. Prabhakaran · R. Pratibha Nalini

Received: 13 March 2010 / Accepted: 12 April 2010 / Published online: 16 July 2010
© Springer-Verlag 2010

Abstract Stable dispersions of micro and nanosized Al_2O_3 particles in ethylene glycol are prepared with the aid of sonication. The temperature dependant acoustic properties such as ultrasonic velocity, adiabatic compressibility, attenuation and acoustic impedance are studied and reported in this paper. In microfluids the particle–fluid interaction is observed to decrease with increase of concentration of particles whereas in nanofluids it is observed to increase up to the critical concentration (0.6 Wt%) and above which the particle–particle interaction dominates due to agglomeration of particles. A range of concentration with significant particle–fluid interaction is identified for effective nanofluid applications.

Keywords Nanofluid · Microfluid · Acoustic properties · Aluminium oxide (Al_2O_3)

1 Introduction

One of the emerging miniaturization techniques is the nanofluid technology which meets the shortcomings of the earlier used bulk fluids and conventional base fluids. Nanofluids exhibit large thermal conductivity compare to traditional (base) fluids and are suitable for heat transfer applications (Choi et al. 2001; Das et al. 2003; Murshed et al. 2005; Xuan and Li 2000). There is a great attraction towards nanofluids because they are proved to be far more superior when compared to the conventional bulk fluids.

Nanofluids offer promising heat transfer applications which is of major importance to industrial sectors including transportation, power generation, micro-manufacturing, electronics, engines, thermal therapy, heating, cooling, ventilation and air conditioning. Many of the reported anomalous enhancements in thermal conductivities in nanofluids were non-reproducible (Kebllinski et al. 2005). Recent experimental studies suggest that nanofluids exhibit thermal conductivity enhancement within Maxwell's limit (Philip et al. 2007; Timofeeva et al. 2007; Eapen et al. 2007; Shima et al. 2009). The studies on viscosity measurements in nanofluids (Prasher et al. 2006; Schmidt et al. 2008; Ayela and Chevalier 2009; Kwak and Kim 2005; Abu-Nada 2009; Xie et al. 2008; Dijke et al. 2009; Lan et al. 2009) show that the shear viscosity increase is much more dramatic than predicted by the Einstein model (Einstein 1906, 1911; Chen et al. 2009). Such increases in viscosity are often attributed to aggregation of nanoparticles.

Though there are few studies made on ultrasonic propagation in magnetic nanofluids by some researchers (Sayan and Ulrich 2002; Motozawa et al. 2008; Raj et al. 2006) no systematic research efforts have been carried out to compare the behaviour of micro and nanofluids in terms of acoustical and thermal parameters. The fundamental understanding of exact mechanisms responsible for the anomalous values of ultrasonic wave propagation is unclear because of the lack of molecular level understanding of the ultrafine particles (Raj et al. 2006) that warrant systematic studies.

A systematic study on the micro and nanofluids is required for the basic understanding of how the nanoparticles behave in fluids and how they interact with each other and with fluid. A comparative analysis between the micro and the nanofluids will enable us to choose fluids with superior properties over conventional fluids.

J. Hemalatha (✉) · T. Prabhakaran · R. Pratibha Nalini
Advanced Materials Lab, Department of Physics, National
Institute of Technology, Tiruchirappalli, Tamilnadu, India
e-mail: hemalatha@nitt.edu

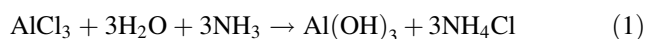
This paper is devoted to the systematic experimental study on the response of suspensions of micro and nano- Al_2O_3 particles in ethylene glycol to the ultrasonic wave propagation. Preparing the stable and homogeneous suspensions of nanoparticles and attaining a deeper understanding of particle–fluid interaction are the main concern. Also the behaviour of Al_2O_3 nanofluid is compared with that of fluid with Al_2O_3 in microscale.

2 Synthesis

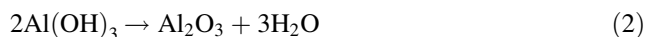
Micro and nanofluids of Al_2O_3 were prepared by dispersing the micro/nanoparticles uniformly in ethylene glycol (EG). The microparticles of Al_2O_3 (of average size 20 μm) and aluminium chloride were purchased from Aldrich. Ethylene glycol, acetone and ammonia solution were purchased from Merck and were used as purchased.

2.1 Nano Al_2O_3 powder

Nanosized Al_2O_3 particles required for the preparation of nanofluids were synthesized in our laboratory through chemical routes. Aluminium chloride was dissolved in aqueous media to obtain a 0.2 M concentration of transparent solution. Then 20 ml of ammonia solution was added as a precipitating agent and the pH of the solution measured before and after the addition of ammonia solution was found to be 2 and 9, respectively. The possible chemical reaction involved in the process described by Eqs. 1 and 2



The slurry, after repeated wash with distilled water and acetone, was filtered. The filtrate was dried in the oven at 80°C, was made into fine powder and then annealed at 1200°C for 2 h to obtain a single phase Al_2O_3 .



2.2 Micro/nanofluids of Al_2O_3

The micro/nanopowders of Al_2O_3 thus obtained were dispersed in ethylene glycol to obtain micro and nanofluids of concentration 0.02, 0.2, 0.4, 0.5, 0.6, 0.7, 0.8 and 1 Wt%. The major problem with the use of microfluids is the rapid settling of the particles which is highly undesirable for many practical heat-transfer/cooling applications. Compared to microparticles, nanoparticles stay suspended much longer due to smaller size. Even then making stable nanofluids is challenging in lab-scale research. But long term stability of the nanofluids could be a practical issue. Long term stability of nanoparticle suspensions is

Table 1 Stability of micro and nanofluids

S. no.	Conc. (Wt%)	Stability (min)	
		Micro	Nano
1	0.02	30	123
2	0.2	8	73
3	0.4	7	65
4	0.5	7	63
5	0.6	6	60
6	0.7	5	51
7	0.8	5	45
8	1	4	28

critical to fully appreciate the benefits of nanofluids (Das et al. 2008).

To achieve uniform dispersion of the particles ultrasonic wave of frequency 4 MHz was passed through the fluid for 35 h with the help of ultrasonic flaw detector apparatus Model Ex 100. It is evident that the ultrasonic treatment to the fluids increases the settling time of the suspension. The stability of the fluids prepared in both micro and nanoscales are observed in terms of settling time and are presented in Table 1.

3 Characterization

Characterization of the nano Al_2O_3 powder was carried out using Fourier transform infrared spectroscopy and X-ray diffraction.

The XRD patterns recorded for the nano Al_2O_3 powder with an X-ray diffractometer (Rigaku Ultima 3) are depicted in Fig. 1. The strong and sharp peaks indicate the crystalline nature of the sample and they match well with the XRD peaks reported earlier by (Sawada 1994; Medraj

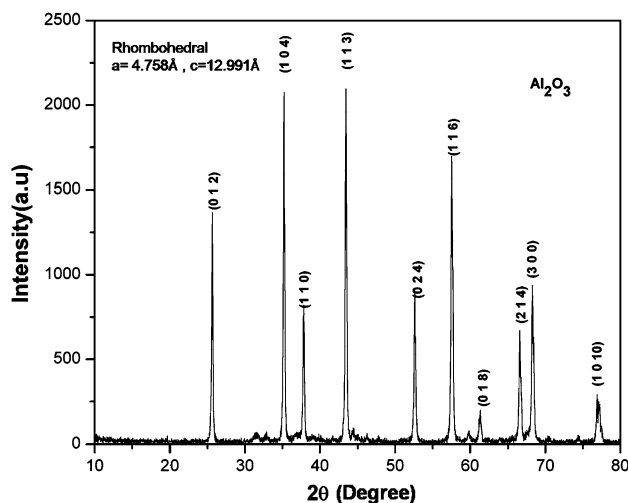


Fig. 1 XRD patterns of nano Al_2O_3

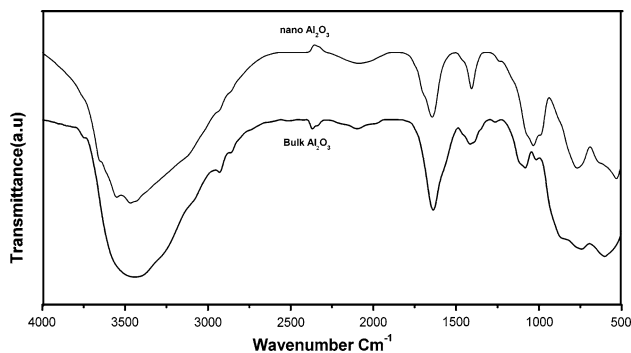


Fig. 2 FTIR spectra of micro and nanoAl₂O₃

et al. 2006). All the reflections are indexed to the rhombohedral unit cell structure of Al₂O₃ (space group *R*3̄*c*, *a* = 4.758 Å and *c* = 12.991 Å) consistent with standard value (JCPDS file no 10-0173). The average particle size was calculated as 43 nm using the Debye–Scherrer formula.

$$D = \frac{0.9\lambda}{\beta \cos \theta} \tag{3}$$

where *D* is the average grain size, λ is wavelength of X-ray (1.541 Å) and β is full width half maximum.

FTIR spectra of the micro and nanoAl₂O₃ powders were obtained using Perkin Elmer (Spectrum RX1) and are presented in Fig. 2. The vibrations of O–H and Al–O bonds generate the observed bands in the infrared region. The broad absorption peaks at 3461 and 1629 cm^{−1} are attributed to the O–H vibration of water. The bands observed at 1035, 750 and 514 cm^{−1} are produced by the Al–O bonds (Vazquez et al. 1997; Shek et al. 1997).

4 Experimental

The velocity values of ultrasonic wave propagation through the micro and nanofluid samples were measured using a single frequency continuous wave ultrasonic interferometer

Table 2 Velocity, density, viscosity and adiabatic compressibility of micro and nanofluids at 30, 40 and 50°C

Temp (°C)	Conc. (Wt%)	<i>C</i> (m/s)		$\rho \times 10^3$ (kg/l)		$\eta \times 10^{-3}$ (Ns/m ²)		$\beta \times 10^{-10}$ (m ² N ^{−1})	
		Micro	Nano	Micro	Nano	Micro	Nano	Micro	Nano
30	0	1648	1648	1.106	1.106	9.760	9.760	3.330	3.330
	0.02	1660	1648	1.106	1.106	5.464	6.464	3.282	3.328
	0.2	1656	1653	1.105	1.104	7.999	8.999	3.300	3.315
	0.4	1651	1670	1.107	1.102	9.411	10.411	3.315	3.254
	0.5	1649	1678	1.108	1.101	10.003	11.018	3.318	3.225
	0.6	1648	1683	1.109	1.100	10.485	11.485	3.321	3.209
	0.7	1646	1682	1.110	1.101	10.789	11.780	3.326	3.210
	0.8	1645	1678	1.110	1.102	10.946	11.946	3.329	3.223
	1	1644	1668	1.111	1.104	11.157	12.157	3.331	3.255
40	0	1619	1619	1.101	1.101	6.494	6.494	3.466	3.466
	0.02	1640	1632	1.110	1.101	5.223	6.223	3.351	3.410
	0.2	1635	1634	1.098	1.096	5.681	6.681	3.407	3.417
	0.4	1633	1648	1.101	1.093	6.296	7.296	3.406	3.369
	0.5	1632	1656	1.103	1.092	6.563	7.554	3.404	3.342
	0.6	1631	1660	1.104	1.091	6.737	7.737	3.406	3.326
	0.7	1629	1659	1.104	1.092	6.808	7.808	3.412	3.326
	0.8	1627	1656	1.104	1.094	6.799	7.799	3.422	3.333
	1	1622	1649	1.104	1.098	6.663	7.663	3.444	3.350
50	0	1596	1596	1.093	1.093	5.891	5.891	3.593	3.593
	0.02	1616	1612	1.077	1.093	3.266	4.266	3.556	3.520
	0.2	1612	1602	1.093	1.088	4.446	5.446	3.521	3.582
	0.4	1607	1623	1.094	1.084	4.620	5.620	3.540	3.502
	0.5	1605	1637	1.094	1.081	4.687	5.678	3.547	3.454
	0.6	1604	1645	1.095	1.079	4.757	5.757	3.550	3.425
	0.7	1603	1644	1.094	1.081	4.802	5.817	3.556	3.423
	0.8	1602	1638	1.093	1.084	4.875	5.875	3.565	3.438
	1	1600	1624	1.091	1.090	5.200	6.200	3.582	3.478

(Model F81, Mittal Enterprises, New Delhi) with an accuracy of $\pm 0.05\%$ at frequency of 2 MHz. The viscosity of the suspensions was carried out by measuring the times of flow of the fluids using Ostwald's viscometer with an accuracy of $\pm 0.2\%$. The density of the fluids was determined using specific gravity bottle (5 cc) with accuracy of ± 2 parts in 10^4 . All these measurements were performed for the fluids of all concentrations at three different temperatures of 30, 40 and 50°C . The constant temperatures were maintained by circulating water from a thermostatically controlled water bath with accuracy of $\pm 0.1^\circ\text{C}$. The velocity, density, viscosity measurements were repeated several times for accuracy and the average of five continuous consistent values are reported in this paper.

5 Results and discussion

The acoustical parameters like adiabatic compressibility (β), attenuation (α/f^2) and acoustic impedance (Z) were measured for both micro and nanofluids using the velocity (C), density (ρ) and viscosity (η) data obtained through the experiments. The adiabatic compressibility of the samples was determined using the Newton–Laplace's relation (Rowlinson and Swinton 1982; Povey 1997)

$$\beta = \frac{1}{\rho C^2} \quad (4)$$

The characteristic acoustic impedance was calculated for all the samples using the relation (Matheson 1971)

$$Z = \rho C \quad (5)$$

The decay of ultrasonic wave while propagation was obtained using Stokes relation (Morse and Ingard 1986) of attenuation

$$\alpha/f^2 = \frac{8\pi^2\eta}{3\rho C^3} \quad (6)$$

The parameters like velocity, density, viscosity and the adiabatic compressibility of micro and nanofluids of various concentrations are listed in Table 2 where the acoustic impedance and attenuation are tabulated in Table 3. Figure 3a and b shows the variations of ultrasonic velocity as a function of concentration and as a function of temperature.

The ultrasonic velocity of micro Al_2O_3 fluid decreases with increase of concentration indicating that the fluids of low concentration are less compressible than those of higher concentration. This can be understood more clearly in terms of increased density and changes in adiabatic compressibility. The decreasing adiabatic compressibility, decreasing acoustic impedance and increasing attenuation

Table 3 Attenuation and acoustic impedance of micro and nanofluids at 30, 40 and 50°C

Temp ($^\circ\text{C}$)	Conc. (Wt%)	$\alpha/f^2 \times 10^{-14}$ (Np/m)		$Z \times 10^3$ (Ns/m ³)	
		Micro	Nano	Micro	Nano
30	0	5.186	5.186	1822	1822
	0.02	2.841	4.474	1835	1823
	0.2	4.187	4.092	1830	1825
	0.4	4.992	3.498	1827	1840
	0.5	5.301	3.282	1827	1848
	0.6	5.555	3.193	1827	1852
	0.7	5.709	3.247	1827	1852
	0.8	5.799	3.412	1826	1849
	1	5.944	3.935	1826	1842
	40	0	3.656	3.656	1782
0.02		2.841	2.870	1820	1797
0.2		3.111	3.124	1795	1791
0.4		3.423	2.787	1798	1801
0.5		3.574	2.609	1800	1807
0.6		3.689	2.549	1800	1811
0.7		3.745	2.648	1799	1812
0.8		3.762	2.867	1796	1812
1		3.718	3.559	1790	1810
50		0	3.487	3.487	1744
	0.02	1.890	2.674	1740	1763
	0.2	2.553	2.405	1762	1743
	0.4	2.675	2.003	1758	1759
	0.5	2.710	1.874	1757	1769
	0.6	2.768	1.811	1756	1775
	0.7	2.811	1.814	1754	1777
	0.8	2.858	1.874	1751	1776
	1	3.072	2.202	1745	1770

shown in Figs. 4 and 5, indicate the weakening of particle–fluid interaction at higher concentrations.

The velocity of nanofluids while observed as a measure of concentration is seen to have a different trend as it increases to a maximum value up to 0.6 Wt% above which it starts decreasing. It is obvious that the reduction of particle size is the major factor that causes the drastic difference in the velocity plot of nanofluid when compared to the microfluid.

The velocity values of the nanofluids are less than those of microfluids until the concentration of 0.24% at 30°C (0.2% at 40°C and 0.3% at 50°C), however, at higher concentrations the values exceed those of microfluid velocity values. The velocity values of nanofluids are highly greater than those in microfluids at a particular concentration of 0.6%.

The possible reasons for the linear increase in the ultrasonic velocity at lower concentrations up to 0.6% of

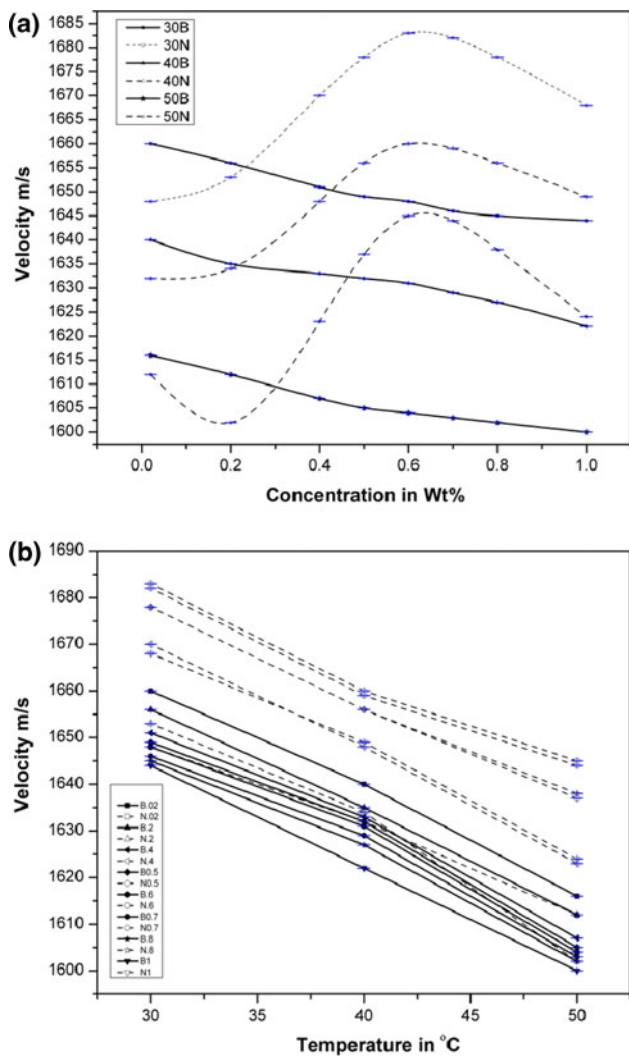


Fig. 3 Plots of ultrasonic velocity versus concentration at various temperatures

these nanofluids are the low values of density and attenuation. The decreasing trend of attenuation is seen in Fig. 5. Moreover, the nanosized alumina has the surface catalytic effect because of the formation of hydrogen bonds with ethylene glycol. It can adsorb more ethylene glycol on its surface due its large surface area and can transport from one point to another point easily. Also, when the nanosized alumina and microsized ethylene glycol molecules interact with each other through secondary forces of attraction, there will be a formation of hierarchical structure which further enhances the velocity.

Thus the decrease in compressibility, increase in viscosity, less density and less attenuation favour higher velocity of the ultrasonic waves at lower concentrations of nanofluids. So it is evident that there is a strong particle–fluid interaction favoring an increase in velocity below the concentration 0.6%.

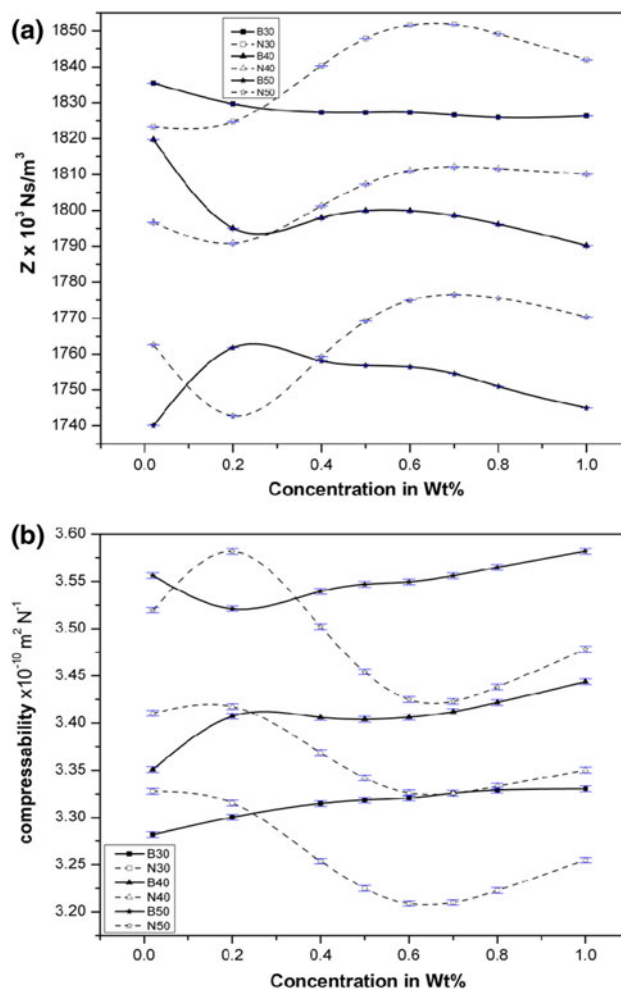


Fig. 4 Compressibility versus concentration and acoustic impedance versus concentration at various temperatures

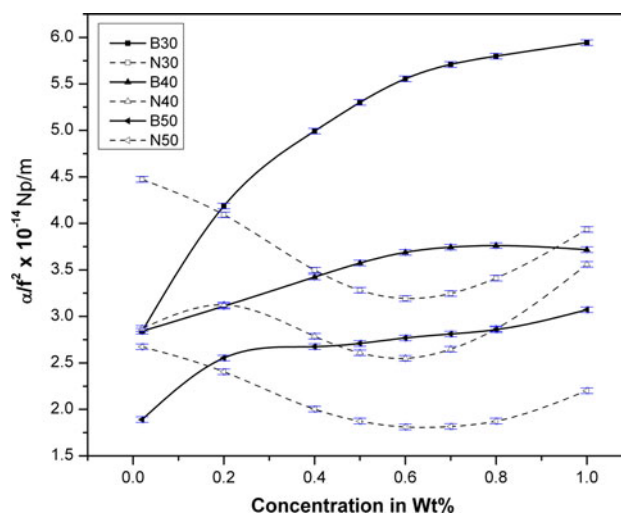


Fig. 5 Attenuation versus concentration for micro and nanofluids at various temperatures

All the aforesaid reasons hold true only up to the critical concentration of 0.6 Wt% of the nanofluid above which the response of the curve shows a change. Above this concentration, the velocity value decreases indicating the decrease in the nanoparticle–fluid interaction and increase of particle–particle interaction. It is understood through all the acoustical parameters that in nanoAl₂O₃–EG fluid the agglomeration starts at 0.6 Wt% and the particle–particle interaction becomes predominant leading to a decrease in the velocity value.

To verify the agglomeration of nanoparticles at higher concentrations, nanofluids of concentrations 0.5, 0.6 and 0.7 Wt% are spin-coated on clean microglass slides with 2000 rpm for 20 s using spin coating unit (DELTASPIN-1). Thin films thus formed on the glass substrate are left for

1 day at room temperature to dry up. Then the film specimens are investigated using Scanning Electron Microscope (JEOL-JSM-6390). As the SEM micrographs are not too helpful to visualize the agglomeration, Field Emission Scanning Electron Micrographs of the samples obtained using JEOL-JSM-6701F are also presented in Fig. 6. The SEM micrographs show the closeness of particles at higher concentrations whereas the high resolution FESEM micrographs manifest the growth in size of the agglomerates.

We may also reason out the behaviour at higher concentrations by observing the increasing compressibility and attenuation values which do not favour the ultrasonic wave propagation. So we can conclude that the concentration range from 0.2 to 0.6% in which the nanoAl₂O₃–fluid

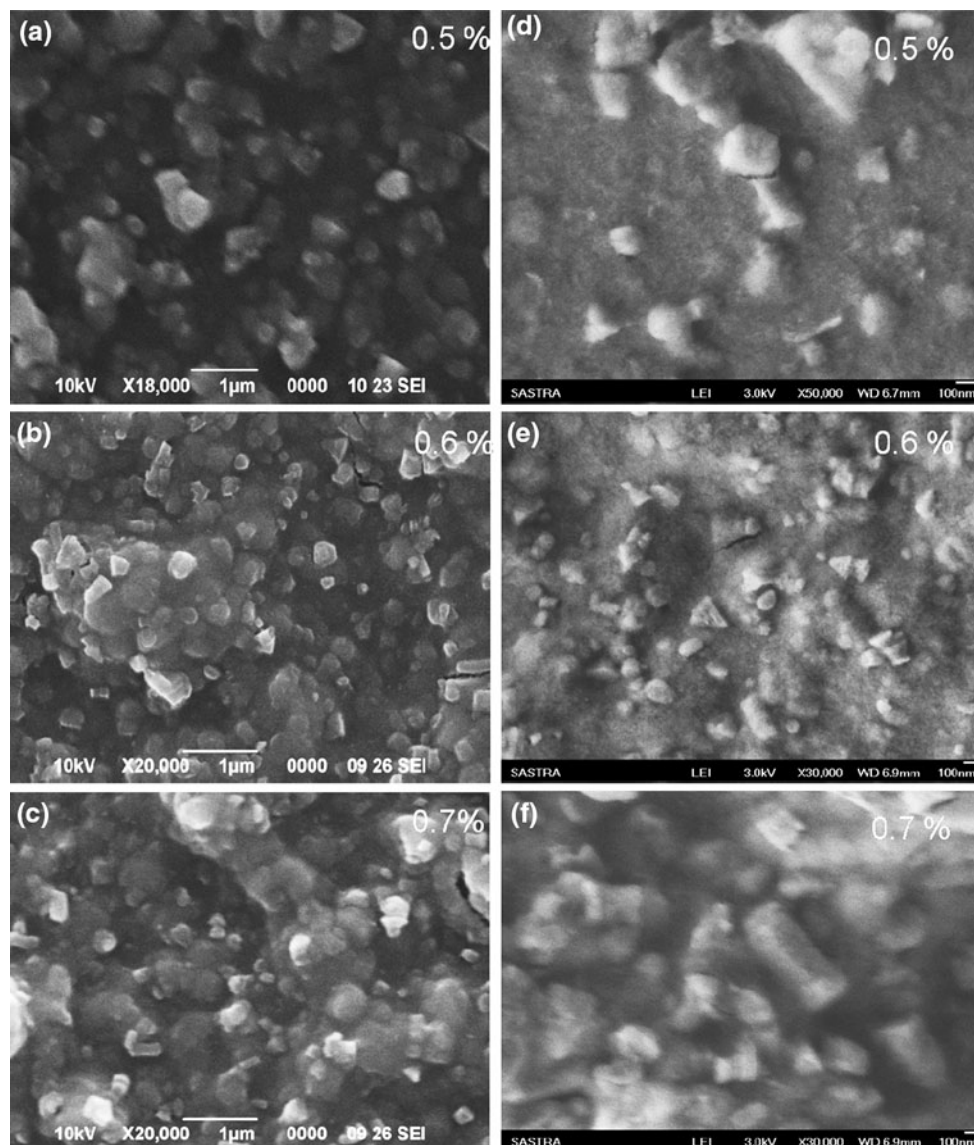


Fig. 6 Particle images acquired using SEM (a–c) and FESEM (d–f)

interaction is significant and is highly suitable for nanofluid applications.

Also, it is clearly seen that the ultrasonic velocity versus temperature plots of micro and nanofluids are linear for all concentrations with a constant slope. $dC/dT \sim -2.2 \text{ m/s } ^\circ\text{C}$. The velocity values decrease with increase of temperature for both micro and nanofluid for all concentrations studied. This is attributed to the increase of compressibility with the temperature which is evident from Fig. 4b. This proves the weakening of the particle–fluid interaction at high temperatures. While increasing the temperature, the intermolecular bonds break and there will be a volume expansion (Tandon and Gambhir 1991) of the constituent molecules which results in decrease in velocity.

6 Conclusion

Homogeneous suspensions of micro and nanosized Al_2O_3 in ethylene glycol were prepared in various concentrations with the help of ultrasonication. The acoustical study including ultrasonic velocity, adiabatic compressibility, attenuation and acoustic impedance was made for all the fluid samples at temperatures 30, 40 and 50°C . The ultrasonic, viscosity and density parameters of micro and nanofluids are compared.

From the analysis of the above parameters it is evident that the particle–fluid interaction in microfluids decreases with increasing particle loading. But for the nanofluids the particle–fluid interaction increases with increase of concentration up to a critical concentration of 0.6 Wt% above which the particle–fluid interaction weakens due to strong particle–particle interaction and thereby agglomeration.

The possible reason is presented below. At low concentration range the inter particle distance is longer and hence the particle–fluid interaction dominates. But at higher concentrations as the inter particle distance decreases due to the availability of more number of particles, the particle–particle interaction is strengthened. The experimental results show that at concentrations above 0.6% the particles come close enough to initiate the agglomeration. FESEM micrographs also prove the same by showing the massive growth of agglomerates at higher concentrations.

The difference in the behaviour of nanofluid from that of microfluid can be attributed to the relatively high surface area to volume ratio of the nanoparticles which is 1000 times larger than that of microparticles. A high proportion of constituent atoms reside on the surface of the nanoparticle as opposed to the interior enabling more surface level interactions with other species like ethylene glycol or $\text{nanoAl}_2\text{O}_3$.

Such particle–fluid interaction studies are helpful to understand the reasons behind anomalous enhancements in physical properties of nanofluids and to realize the mechanism of fluid flow in nanoscale. The knowledge of which will help to improve the performance of nanofluids in MEMS devices and other practical applications.

References

- Abu-Nada E (2009) Effects of variable viscosity and thermal conductivity of Al_2O_3 –water nanofluid on heat transfer enhancement in natural convection. *Int J Heat fluid flow* 30:679–690
- Ayela F, Chevalier J (2009) Comment on particle concentration and tube size dependence of viscosities of Al_2O_3 –water nanofluids flowing through micro- and minitubes. *Appl Phys Lett* 94: 066101
- Chen H, Ding Y, Lapkin A, Fan X (2009) Rheological behaviour of ethylene glycol–titanate nanotube nanofluids. *J Nanopart Res* 11:1513–1520
- Choi SUS, Zhang ZG, Yu W, Lockwood FE, Grukle EA (2001) Anomalous thermal conductivity enhancement in nano-tube suspensions. *Appl Phys Lett* 79:2252–2254
- Das SK, Putra N, Thiesen P, Roetzel W (2003) Temperature dependence of thermal conductivity enhancement for nanofluids. *J Heat Transfer* 125:567–574
- Das SK, Choi Stephen US, Yu W, Pradeep T (2008) *Nanofluids: science and technology*. Wiley, New Jersey
- Dijke KV, Kobayashi I, Schroën K, Uemura K, Nakajima M, Boom R (2009) Effect of viscosities of dispersed and continuous phases in microchannel oil-in-water emulsification. *Microfluid Nanofluid*. doi:10.1007/s10404-009-0521-7
- Eapen J, Williams WC, Buongiorno J, Hu L, Yip S, Rusconi R, Piazza R (2007) Mean-field versus microconvection effects in nanofluid thermal conduction. *Phys Rev Lett* 99:095901
- Einstein A (1906) Eine neue Bestimmung der Molekuldimension (a new determination of the molecular dimensions). *Ann Phys* 19(2):289–306
- Einstein A (1911) Berichtigung zu meiner Arbeit: Eine neue Bestimmung der Molekul-dimension (correction of my work: a new determination of the molecular dimensions). *Ann Phys* 34(3):591–592
- Kebllinski P, Eastman JA, Cahill DG (2005) Nanofluid for thermal transport. *Mater Today* 8:36–44
- Kwak K, Kim C (2005) Viscosity and thermal conductivity of copper oxide nanofluid dispersed in ethylene glycol. *Korea-Aust Rheol J* 17(2):35–40
- Lan WJ, Li SW, Xu JH, Luo GS (2009) Rapid measurement of fluid viscosity using co-flowing in a co-axial microfluidic device. *Microfluid Nanofluid*. doi:10.1007/s10404-009-0540-4
- Matheson AJ (1971) *Molecular acoustics*. Wiley, New York
- Medraj M, Hammond R, Parvez MA, Drew RAL, Thompson WT (2006) High temperature neutron diffraction study of the Al_2O_3 – Y_2O_3 system. *J Eur Ceram Soc* 26:3515–3524
- Morse PM, Ingard KU (1986) *Theoretical acoustics*. Princeton University Press, New Jersey
- Motozawa M, Iizuka Y, Sawada T (2008) Experimental measurements of ultrasonic propagation velocity and attenuation in a magnetic fluid. *J Phys Condens Matter* 20:204117. doi:10.1088/0953-8984/20/20/204117
- Murshed SMS, Leong KC, Yang C (2005) Enhanced thermal conductivity of TiO_2 –water based nanofluids. *Int J Therm Sci* 44:367–373

- Philip J, Shima PD, Raj B (2007) Experimental evidence for enhancement of thermal conductivity under clustering. *Appl Phys Lett* 91:203108
- Povey MJW (1997) *Ultrasonic techniques for fluids characterization*. Academic Press, USA, p 25
- Prasher R, Song D, Wang J, Phelan P (2006) Measurements of nanofluid viscosity and its implications for thermal applications. *Appl Phys Lett* 89:133108. doi:[10.1063/1.2356113](https://doi.org/10.1063/1.2356113)
- Raj B, Philip J, Rajkumar KV, Kalyanasundaram P (2006) Effect of magnetic field on ultrasonic velocity in a magnetic nanofluid. *Proc Indian Natl Sci Acad* 72:145–151
- Rowlinson JS, Swinton FL (1982) *Liquid and liquid mixtures*, 3rd edn. Butterworths, London, pp 16–17
- Sawada H (1994) Residual electron density study of α -aluminum oxide through refinement of experimental atomic scattering factors. *Mater Res Bull* 29(2):127–133
- Sayan P, Ulrich J (2002) The effect of particle size and suspension density on the measurement of ultrasonic velocity in aqueous solutions. *Chem Eng Process* 41:281–287
- Schmidt AJ, Chiesa M, Torchinsky DH, Johnson JA, Boustani A, McKinley GH, Nelson KA, Chen G (2008) Shear and longitudinal viscosity of nanoparticle suspension in insulating media. *Appl Phys Lett* 92:244107 (1–3)
- Shek LH, Lai KL, Gu TS, Lin GM (1997) Transformation evolution and infrared absorption spectra of amorphous and crystalline nano- Al_2O_3 powders. *Nanostruct Mater* 8:605–610
- Shima PD, Philip J, Raj B (2009) Role of microconvection induced by Brownian motion of nanoparticles in the enhanced thermal conductivity of stable nanofluids. *Appl Phys Lett* 94:223101
- Tandon SP, Gambhir S (1991) Effect of temperature on ultrasonic velocity in aqueous solutions of rare-earth chlorides. *Acustica* 75:190–192
- Timofeeva EV, Gavrilov AN, McCloskey JM, Tolmachev YV (2007) Thermal conductivity and particle agglomeration in alumina nanofluids: experiment and theory. *Phys Rev E* 76:061203-1–061203-16
- Vazquez A, Lopez T, Gomez R, Bokhimi X, Morales A, Novaro O (1997) X-ray diffraction, FTIR, and NMR characterization of sol-gel alumina doped with lanthanum and cerium. *J Solid State Chem* 128:161–168
- Xie H, Chen L, Wu Q (2008) Measurements of the viscosity of suspensions (nanofluids) containing nanosized Al_2O_3 particles. *High Temp High Press* 37:127–135
- Xuan Y, Li Q (2000) Heat transfer enhancement of nanofluids. *Int J Heat Fluid Flow* 21:58–64